

Probing flavor changing interactions in photon-photon collisions ^{*}

Jiang Yi^b, Zhou Mian-Lai^b, Ma Wen-Gan^{a,b,c}, Han Liang^b, Zhou Hong^b and Han Meng^b

^aCCAST (World Laboratory), P.O.Box 8730, Beijing 100080, China.

^bDepartment of Modern Physics, University of Science and Technology of China (USTC), Hefei, Anhui 230027, China.

^cInstitute of Theoretical Physics, Academia Sinica, P.O.Box 2735, Beijing 100080, China.

Abstract

We examine the subprocess $\gamma\gamma \rightarrow t\bar{c} + \bar{t}c$ at electron-positron colliders in the two-Higgs-doublet model with flavor-changing scalar couplings, where all the one-loop contributions are considered, and the results are applicable to the whole mass range of the weakly coupled Higgs bosons. Because of the heavy top quark mass, this process is important in probing the flavor-changing top-charm-scalar vertex and could be detectable at the Next Linear Collider, if the values of the parameters are favorable. The results show that this process is more promising than the direct e^+e^- process for discovering flavor changing scalar interactions.

PACS number(s):13.65.+i, 11.30.Hv, 12.60.Fr, 14.65.Ha

^{*}This work was supported by National Natural Science Foundation of China

I. Introduction

The experimental data have shown that the flavor changing scalar interactions (FCSI) involving the light quarks are strongly suppressed. This leads to the suppression of the flavor changing neutral currents(FCNC) which is an important feature of the standard model(SM) which was explained in terms of the GIM mechanism. In the commonly used two-Higgs-doublet models(THDM), the absence of the FCSI at the tree level can be assured, if the natural flavor conservation(NFC) condition[1] is valid, by imposing discrete symmetries on the model. Then the THDM model with NFC condition can be subdivided into two modes, i.e., Model I and Model II. In Model I, both the up and down type quarks get their masses from the same Higgs doublet, and in Model II the quarks get their masses from different doublets. Two years ago the CDF and D0 collaborations found that the top quark has a very large mass (world average value: $m_t = 175.6 \pm 5.5 \text{ GeV}$)[2]. This extraordinary mass scale of the top quark has many important implications pertaining to many outstanding issues in theoretical particle physics. One of these consequences is that FCSI at the tree level would exist at high mass scales. The measurement of FCSI involving top quark would provide an important test for the discrimination of various models. As Cheng, Sher and other authors[3][4][5][6] pointed out, since the Yukawa couplings are typically related to the masses of the fermions participating at the vertices, it is rather natural to expect having Yukawa couplings for the FCSI instead of placing the constraints due to NFC on the theory. If the Yukawa couplings are proportional to the quark masses, low energy limits on FCNC's may be evaded because the flavor changing couplings to the light quarks are small, and the

suppression of the FCSI involving light quarks can be automatically satisfied. Then the imposition of discrete symmetries to insure that the NFC condition is satisfied, which is normally invoked in commonly used two-Higgs-doublet models to prevent the FCSI at the tree level, is therefore unnecessary. We call such THDM as the third mode of THDM(i.e., THDM III) [6]. In the framework of this model the effects of FCSI involving the heavy quark will be enhanced.

If the philosophy of the THDM III is correct, one would expect that large effects of the FCSI could manifest themselves in the cases involving the massive top quark. Therefore testing the existence of the flavor changing scalar interactions involving top quarks is a promising task for future colliders. Recently, D. Atwood et al. [7] presented results of a calculation for the process $e^+e^- \rightarrow t\bar{c}$ (or $\bar{t}c$) in the THDM III, and they got R^{tc}/λ^4 to be in the order of 10^{-5} with proper parameters. They stressed that this experimental signal is very clean and that FCSI can lead to measurable effects. As we know, the future Next Linear Collider(NLC) is designed as a $500 \text{ GeV } e^+e^-$ collider with an integral luminosity of the order of 10 fb^{-1} per year. There is also a possibility that the NLC may be operated in $\gamma\gamma$ collision mode, then it provides another facility in top physics research with a cleaner environment. The subprocess $\gamma\gamma \rightarrow h^0, A^0 \rightarrow t\bar{c} + \bar{t}c$ was first studied by Hou and Lin[8]. They pointed out that at the NLC we can also use this process to study FCSI. There they presented results of calculations for the specific case where on-mass-shell neutral Higgs bosons with the masses in the range $200 \text{ GeV} < m_{h^0, A^0} < 2 m_t \simeq 350 \text{ GeV}$ are produced from $\gamma\gamma$ fusion and the photon helicities have the average value $\langle \lambda\lambda' \rangle \sim +1$. They predicted that one can get $10^2 \sim 10^3$ raw events per year with 50 fb^{-1} luminosities in NLC operated in $\gamma\gamma$ collision

mode.

In this paper we present the complete one-loop calculation for the subprocess $\gamma\gamma \rightarrow t\bar{c}$ (or $\bar{t}c$) at the $O(m_t m_c/m_W^2)$ order in the THDM III, and the results are applicable to the whole mass range for weakly coupled Higgs bosons. The production rates of $e^+e^- \rightarrow \gamma\gamma \rightarrow t\bar{c} + \bar{t}c$ are also given for the NLC energy range. It shows that this process is more promising than the straight e^+e^- process for probing FCSI. The paper is organized as follows: The details of calculation are given in Sec. II. In Sec. III there are numerical results and discussion and a short summary. Finally, the explicit expressions used in the paper are collected in appendix.

II. Calculation

In the third type of the two-Higgs-doublet model, the up-type and down-type quarks are allowed simultaneously to couple to more than one scalar doublet. We consider the THDM has two scalar $SU(2)_w$ doublets, ϕ_1 and ϕ_2 :

$$\phi_1 = \begin{pmatrix} \phi_1^+ \\ \phi_1^0 \end{pmatrix}, \quad \phi_2 = \begin{pmatrix} \phi_2^+ \\ \phi_2^0 \end{pmatrix}, \quad (1)$$

with Lagrangian

$$\mathcal{L}_\phi = D^\mu \phi_1^+ D_\mu \phi_1 + D^\mu \phi_2^+ D_\mu \phi_2 - V(\phi_1, \phi_2), \quad (2)$$

where $V(\phi_1, \phi_2)$ is the general potential which is consistent with the gauge symmetries. Since there is no global symmetry that distinguishes the two doublets in THDM III, we can assume that

$$\langle \phi_1 \rangle = \begin{pmatrix} 0 \\ v/\sqrt{2} \end{pmatrix}, \quad \langle \phi_2 \rangle = 0 \quad (3)$$

where $v \simeq 246 \text{ GeV}$. The physical spectrum of Higgs bosons consists of two scalar neutral bosons h^0 and H^0 , one pseudoscalar neutral boson A^0 and two charged Higgs H^\pm ,

$$\begin{aligned} H^0 &= \sqrt{2}[(\text{Re}\phi_1^0 - v) \cos \alpha + \text{Re}\phi_2^0 \sin \alpha], \\ h^0 &= \sqrt{2}[-(\text{Re}\phi_1^0 - v) \sin \alpha + \text{Re}\phi_2^0 \cos \alpha], \\ A^0 &= \sqrt{2}(-\text{Im}\phi_2^0). \end{aligned} \quad (4)$$

The masses of the five neutral and charged Higgs bosons and the mixing angle α are free parameters of the model. The Yukawa couplings to quarks are[9],

$$\mathcal{L}_Y^Q = \lambda_{ij}^U \bar{Q}_i \tilde{\phi}_1 U_j + \lambda_{ij}^D \bar{Q}_i \phi_1 D_j + \xi_{ij}^U \bar{Q}_i \tilde{\phi}_2 U_j + \xi_{ij}^D \bar{Q}_i \phi_2 D_j, \quad (5)$$

where the first two terms give masses of the quark mass eigenstates, and ξ_{ij}^U and ξ_{ij}^D are the 3×3 matrices which give the strength of the flavor changing neutral scalar vertices. The ξ s are all free parameters and can be constrained by the experimental data. If we neglect CP violation, the ξ s are all real. In this paper we use the Cheng-Sher Ansatz(CSA)[5] and let

$$\xi_{ij} \sim \frac{\sqrt{m_i m_j}}{v}.$$

And we can parametrize the Yukawa couplings as

$$\xi_{ij} = g \frac{\sqrt{m_i m_j}}{m_W} \lambda. \quad (6)$$

Comparing it with the usual gauge couplings of $SU(2) \times U(1)$, one has $\lambda = \frac{1}{\sqrt{2}}$. In our calculation we use $\lambda = \frac{1}{\sqrt{2}}$ and note that there is no stringent bound on the coupling factor λ theoretically.

This process can be produced via one-loop diagrams, and the Feynman diagrams are given in figure 1(a) and figure 1(b), where the contribution of neutral Higgs and charged

Higgs one-loop diagrams are given respectively. The diagrams exchanging the two external $\gamma\gamma$ lines are not shown in Fig.1(a) and Fig.1(b). Fig.1(a)(1 ~ 12) and Fig. 1(b)(1 ~ 6) are the self-energy diagrams, Fig. 1(a)(13 ~ 20) and Fig. 1(b)(7 ~ 10, 13 ~ 16) are the vertex correction diagrams, Fig. 1(a)(25 ~ 28) are the s-channel diagrams, Fig.1(b)(19) is the quartic vertex diagram and Fig. 1(a)(20 ~ 24) and Fig. 1(b)(11 ~ 12, 17 ~ 18, 20 ~ 21) are the box diagrams. There is no tree-level contribution, therefore the proper vertex counterterm cancels the counterterms of the diagrams with external legs. That is to say the evaluation can be simply carried out by summing all unrenormalized reducible and irreducible diagrams.

To simplify the calculation we set $\alpha = 0$ as adopted in Refs.[7] and [9] and let all scalar bosons be degenerate, i.e., $m_{h^0} = m_{A^0} = m_{H^\pm} = M_s$ where M_s is the common scalar mass. The contribution from the coupling involving H^0 is suppressed due to $\alpha = 0$.

In the calculation for the s-channel diagrams(Fig.1.(a)(25 ~ 26)), we take into account the width effects of the h^0 and A^0 propagators. As we know, the decays of h^0 to WW and ZZ are suppressed, because of the factor $\sin \alpha$ in the $h^0 WW$, and $h^0 ZZ$ couplings and h^0 decay to $A^0 A^0$ is also forbidden due to the case of the degenerate masses of h^0 and A^0 . Note that the pseudoscalar A^0 does not couple with gauge boson pair. Therefore only the decays of h^0 and A^0 to final states $q_i \bar{q}_j$ need to be considered, where q_i and q_j represent quarks of flavor i and j respectively. The decay width for the scalar h^0 can be written as[10]

$$\Gamma(h^0 \rightarrow q\bar{q}) = \frac{3g^2 m_{h^0}}{32\pi M_W^2} m_q \left(1 - 4m_q^2/m_{h^0}^2\right)^{3/2}$$

and

$$\Gamma(h^0 \rightarrow t\bar{c} + \bar{t}c) = \frac{3g^2 m_{h^0}}{32\pi M_W^2} \cdot 2m_t m_c \left[1 - (m_t + m_c)^2/m_{h^0}^2\right]^{3/2} \times \left[1 - (m_t - m_c)^2/m_{h^0}^2\right]^{1/2}. \quad (7)$$

The decay width for the pseudoscalar A^0 boson can be represented by exchanging exponents $3/2 \leftrightarrow 1/2$ and $m_{h^0} \leftrightarrow m_{A^0}$ in Eq.(7). When $m_t + m_c < M_s < 2m_t$, the dominant decay modes of h^0 and A^0 are $h^0, A^0 \rightarrow c\bar{c}, b\bar{b}, t\bar{c} + \bar{t}c$, whereas when $M_s > 2m_t$, the final state $t\bar{t}$ decay channel is open, and their decay widths are rather large due to the large masses of M_s and m_t .

We denote θ as the scattering angle between one of the photons and the final top quark. Then in the center-of-mass(CMS) we express all the four-momenta of the initial and final particles by means of the total energy $\sqrt{\hat{s}}$ and the scattering angle θ . The four-momenta of top quark and charm quark are p_1 and p_2 respectively and they read

$$\begin{aligned} p_1 &= \left(E_t, \sqrt{E_t^2 - m_t^2} \sin\theta, 0, \sqrt{E_t^2 - m_t^2} \cos\theta \right), \\ p_2 &= \left(E_c, -\sqrt{E_c^2 - m_c^2} \sin\theta, 0, -\sqrt{E_c^2 - m_c^2} \cos\theta \right), \end{aligned} \quad (8)$$

where

$$E_t = \frac{1}{2} \left(\sqrt{\hat{s}} + (m_t^2 - m_c^2)/\sqrt{\hat{s}} \right), \quad E_c = \frac{1}{2} \left(\sqrt{\hat{s}} - (m_t^2 - m_c^2)/\sqrt{\hat{s}} \right). \quad (9)$$

p_3 and p_4 are the four-momenta of the initial γ and they are

$$p_3 = \left(\frac{1}{2}\sqrt{\hat{s}}, 0, 0, \frac{1}{2}\sqrt{\hat{s}} \right), \quad p_4 = \left(\frac{1}{2}\sqrt{\hat{s}}, 0, 0, -\frac{1}{2}\sqrt{\hat{s}} \right). \quad (10)$$

The corresponding matrix element for all the diagrams in figure 1(a) and figure 1(b) is written as

$$M = M^{\hat{s}} + M^{\hat{t}} + M^{\hat{u}} \quad (11)$$

The upper indexes \hat{s} , \hat{t} , and \hat{u} represent the amplitudes corresponding to the s-channel diagrams, t-channel and u-channel diagrams in figure 1(a) and figure 1(b) respectively. The variables \hat{s} , \hat{t} and \hat{u} are usual Mandelstam variables in the center of mass system of $\gamma\gamma$. Their definitions are:

$$\begin{aligned}\hat{s} &= (p_1 + p_2)^2 = (p_3 + p_4)^2, & \hat{t} &= (p_1 - p_3)^2 = (p_2 - p_4)^2, \\ \hat{u} &= (p_1 - p_4)^2 = (p_2 - p_3)^2.\end{aligned}\quad (12)$$

We collect all the explicit expressions of the amplitudes appearing in equation (11) in the appendix. The total cross section for $\gamma\gamma \rightarrow t\bar{c} + \bar{t}c$ can be written in the form

$$\hat{\sigma}(\hat{s}) = \frac{2N_c}{16\pi\hat{s}^2} \int_{\hat{t}^-}^{\hat{t}^+} d\hat{t} |\bar{M}|^2 \quad (13)$$

where $|\bar{M}|^2$ is the initial spin-averaged matrix element squared, the color factor $N_c = 3$ and $\hat{t}^\pm = 1/2(m_t^2 + m_c^2 - \hat{s}) \pm \sqrt{E_t^2 - m_t^2} \sqrt{\hat{s}}$. The total cross section for $e^+e^- \rightarrow \gamma\gamma \rightarrow t\bar{c} + \bar{t}c$ can be obtained by folding the $\hat{\sigma}$, the cross section for $\gamma\gamma \rightarrow t\bar{c} + \bar{t}c$, with the photon luminosity,

$$\sigma(s) = \int_{(m_t+m_c)/\sqrt{s}}^{x_{max}} dz \frac{dL_{\gamma\gamma}}{dz} \hat{\sigma} \quad (\gamma\gamma \rightarrow t\bar{c} + \bar{t}c \text{ at } \hat{s} = z^2 s), \quad (14)$$

where \sqrt{s} and $\sqrt{\hat{s}}$ are the e^+e^- and $\gamma\gamma$ CMS energies respectively, and the quantity $dL_{\gamma\gamma}/dz$ is the photon luminosity, which is defined as

$$\frac{dL_{\gamma\gamma}}{dz} = 2z \int_{z^2/x_{max}}^{x_{max}} \frac{dx}{x} F_{\gamma/e}(x) F_{\gamma/e}(z^2/x). \quad (15)$$

For unpolarized initial electrons and laser photon beams, the energy spectrum of the back-scattered photon is given by[11]

$$F_{\gamma/e} = \frac{1}{D(\xi)} \left[1 - x + \frac{1}{1-x} - \frac{4x}{\xi(1-x)} + \frac{4x^2}{\xi^2(1-x)^2} \right], \quad (16)$$

where

$$D(\xi) = \left(1 - \frac{4}{\xi} - \frac{8}{\xi^2}\right) \ln(1 + \xi) + \frac{1}{2} + \frac{8}{\xi} - \frac{1}{2(1 + \xi)^2}, \quad (17)$$

and $\xi = 4E_0\omega_0/m_e^2$. m_e and E_0 are the mass and energies of the incident electron, respectively. The dimensionless parameter x represents the fraction of the energy of the incident electron carried by the back-scattered photon. In our evaluation, we choose ω_0 such that it maximizes the back-scattered photon energy without spoiling the luminosity by e^+e^- pair production. Then we can get $\xi = 2(1 + \sqrt{2}) \simeq 4.8$, $x_{max} \simeq 0.83$ and $D(\xi) \simeq 1.8$. That is a usual method which was used in Ref.[12].

III. Numerical Results and Discussion

In the numerical evolution we take the input parameters[13] as $m_b = 4.5GeV$, $m_c = 1.35GeV$, $m_t = 175GeV$, $M_W = 80.2226GeV$, $G_F = 1.166392 \times 10^{-5}(GeV)^{-2}$ and $\alpha = 1/137.036$.

Figure 2 shows the cross sections for $\gamma\gamma \rightarrow t\bar{c} + \bar{t}c$ as a function of the masses of the Higgs bosons M_s . The cross sections are displayed for the three values of the $\gamma\gamma$ CMS energy 200 GeV, 400 GeV and 500 GeV respectively. Because there is no stringent bound on the Higgs bosons masses, we choose M_s in the range from 50 GeV to 800 GeV. The higher peak of each curve comes from s-channel resonance effects, where $M_s = m_{h^0} = m_{A^0} \sim \sqrt{\hat{s}}$. The smaller peak of each curve mainly comes from the contribution of the quartic vertex diagram. For the curve $\sqrt{\hat{s}} \sim 200 GeV$, it is located at about $\sqrt{\hat{s}} \sim 2 M_s$, whereas for $\sqrt{\hat{s}} \sim 400 GeV$ and 500 GeV, they are at $M_s \sim 150GeV$. From these curves we find that the cross section can be obviously enhanced when M_s gets close to $\sqrt{\hat{s}}$.

Figure 3 shows the cross sections of $\gamma\gamma \rightarrow t\bar{c} + \bar{t}c$ as a function of $\sqrt{\hat{s}}$, and the three curves correspond to the M_s values 100 GeV, 250 GeV and 500 GeV respectively. For $M_s = 100\text{GeV}$, the effects of the widths of the Higgs bosons are not obvious, and s-channel resonance effects are suppressed, since $\sqrt{\hat{s}}$ is far away from M_s . Therefore its cross section goes down as $\sqrt{\hat{s}}$ increasing. When $\sqrt{\hat{s}}$ approaches the value of M_s , such as $M_s = 250\text{GeV}$, the cross section will be enhanced by the s-channel resonance effects, and the width effects become larger, since the $h^0, A^0 \rightarrow t\bar{c} + \bar{t}c$ channels are opened. The small peak of the dashed line, where $\sqrt{\hat{s}} \sim 2m_t = 350\text{ GeV}$, comes from the contribution of the neutral Higgs box diagrams. For $M_s = 500\text{GeV}$, the cross section goes up from $\sqrt{\hat{s}} \simeq 300\text{GeV}$ due to the s-channel resonance effects and large width effects of h^0 and A^0 .

In figure 4 we show the cross section of $e^+e^- \rightarrow \gamma\gamma \rightarrow t\bar{c} + \bar{t}c$ as a function of center-of-mass energy of electron-positron system \sqrt{s} . The cross section may reach 0.11 femptobarn when $M_s = 250\text{ GeV}$ and $\sqrt{s} = 355\text{ GeV}$. For $M_s = 100\text{GeV}$ the cross section is two orders smaller than that for $M_s = 250\text{ GeV}$. When $M_s = 500\text{ GeV}$, the cross section is only of the order 10^{-4} femptobarn. For a 500 GeV NLC operating in e^+e^- mode with 50 fb^{-1} integrated luminosity, one can expect about 6 raw events when $M_s = 250\text{ GeV}$. Since the cross section of this process roughly scales as λ^4 , if we let $\lambda \simeq 1$, the cross section will be 4 times larger. That is to say about 24 raw events may be produced per year in unpolarized photon collisions. That means the $t\bar{c}$ production may be detectable in future NLC experiment. In Ref.[8] Hou et al. pointed out that one could expect $10^2 \sim 10^3$ $\gamma\gamma \rightarrow h^0, A^0 \rightarrow t\bar{c} + \bar{t}c$ raw events a year with 50 fb^{-1} integrated luminosity, where they assume that the on-mass-shell

neutral Higgs bosons with $200 \text{ GeV} < m_{h^0, A^0} < 2 m_t \simeq 350 \text{ GeV}$ are produced and the photon polarizations have $\langle \lambda\lambda' \rangle \sim +1$. This estimate doesn't contradict ours, if we make the same assumptions and the parameters have their most favorable values. For the process $e^+e^- \rightarrow t\bar{c} + \bar{t}c$, Atwood et al. got $R^{tc} \equiv \frac{\sigma(e^+e^- \rightarrow t\bar{c} + \bar{t}c)}{\sigma(e^+e^- \rightarrow \gamma^* \rightarrow \mu^+\mu^-)} \lesssim few \times 10^{-5}$ [7], when all the masses of Higgs bosons are degenerate, which amounts to less than 0.1 event for a 500 GeV NLC with 50 fb^{-1} integrated luminosity. It shows clearly that with the same parameters, the process $e^+e^- \rightarrow \gamma\gamma \rightarrow t\bar{c} + \bar{t}c$ occurs with larger cross section than $e^+e^- \rightarrow t\bar{c} + \bar{t}c$ process.

In summary, from our one-loop calculation, we can conclude that it is possible in the NLC that the process $e^+e^- \rightarrow \gamma\gamma \rightarrow t\bar{c} + \bar{t}c$ can be used to probe the flavor changing interactions in the context of THDM III with clean signals. The NLC operating in photon-photon mode can produce more events for discovering flavor changing scalar interactions than in electron-positron collision mode.

One of the authors, Ma Wen-Gan, would like to thank the Institute of Theoretical Physics of the University of Vienna and the Institute of High Energy Physics of the Austrian Academy of Sciences for warm hospitality extended to him during his stay under agreement of the exchange program(Project number IV.B.12).

Appendix

We adopt the same definitions of one-loop A, B, C and D integral functions as in Ref.[14]

and the references therein. The dimension $D = 4 - \epsilon$. The integral functions are defined as

$$\begin{aligned}
A_0(m) &= -\frac{(2\pi\mu)^{4-D}}{i\pi^2} \int d^D q \frac{1}{[q^2 - m^2]}, \\
\{B_1; B_\mu; B_{\mu\nu}\}(p, m_1, m_2) &= \frac{(2\pi\mu)^{4-D}}{i\pi^2} \int d^D q \frac{\{1; q_\mu; q_{\mu\nu}\}}{[q^2 - m_1^2][(q+p)^2 - m_2^2]}, \\
\{C_0; C_\mu; C_{\mu\nu}; C_{\mu\nu\rho}\}(p_1, p_2, m_1, m_2, m_3) &= -\frac{(2\pi\mu)^{4-D}}{i\pi^2} \\
&\times \int d^D q \frac{\{1; q_\mu; q_{\mu\nu}; q_{\mu\nu\rho}\}}{[q^2 - m_1^2][(q+p_1)^2 - m_2^2][(q+p_1+p_2)^2 - m_3^2]}, \\
\{D_0; D_\mu; D_{\mu\nu}; D_{\mu\nu\rho}; D_{\mu\nu\rho\alpha}\}(p_1, p_2, p_3, m_1, m_2, m_3, m_4) &= \frac{(2\pi\mu)^{4-D}}{i\pi^2} \\
&\times \int d^D q \{1; q_\mu; q_{\mu\nu}; q_{\mu\nu\rho}; q_{\mu\nu\rho\alpha}\} \\
&\times \{[q^2 - m_1^2][(q+p_1)^2 - m_2^2][(q+p_1+p_2)^2 - m_3^2][(q+p_1+p_2+p_3)^2 - m_4^2]\}^{-1}.
\end{aligned}$$

In our calculation we take the strange quark mass $m_s = 0$. The $M^{\hat{s}}$ in equation (11) can be written as

$$\begin{aligned}
M^{\hat{s}} &= \frac{ig^2 e^2}{36\pi^2 M_W^2} m_t \sqrt{m_t m_c} \epsilon_\mu(p_3) \epsilon_\nu(p_4) \bar{u}(p_1) \\
&\cdot \{2a_{h^0} m_t^2 (C_0 + 4C_{22} - 4C_{23}) [p_3, -p_1 - p_2, m_t, m_t, m_t] (p_1^\mu p_1^\nu + p_1^\mu p_2^\nu + p_1^\nu p_2^\mu + p_2^\mu p_2^\nu) \\
&+ 2a_{h^0} m_t^2 (B_0 [-p_1 - p_2, m_t, m_t] - ((p_1 + p_2) \cdot p_3 C_0 \\
&+ 4C_{24})) [p_3, -p_1 - p_2, m_t, m_t, m_t] + 9[m_b^2 C_0 + m_t m_c (C_{11} - C_{12}) + m_t^2 C_{12} \\
&- \gamma_5 (m_b^2 C_0 - m_t m_c (C_{11} - C_{12}) - m_t^2 C_{12})] [p_2, -p_1 - p_2, m_b, M_s, M_s] g^{\mu\nu} \\
&+ 2ia_{A^0} m_t^2 C_0 [p_3, -p_1 - p_2, m_t, m_t, m_t] \epsilon^{\mu\nu\alpha\beta} \gamma_5 (p_1^\alpha p_3^\beta + p_2^\alpha p_3^\beta) \} v(p_2),
\end{aligned} \tag{A.1}$$

where

$$a_{h^0} = \frac{1}{\hat{s} - m_{h^0}^2 + i\Gamma_{h^0} m_{h^0}}, \quad a_{A^0} = \frac{1}{\hat{s} - m_{A^0}^2 + i\Gamma_{A^0} m_{A^0}}.$$

The amplitude of $M^{\hat{t}}$ can be written as

$$\begin{aligned}
M^{\hat{t}} = & \frac{ig^2 e^2}{288\pi^2 M_W^2} \sqrt{m_t m_c} \epsilon_\mu(p_3) \epsilon_\nu(p_4) \bar{u}(p_1) (f_1 p_1^\mu p_1^\nu + f_2 p_1^\mu p_2^\nu + f_3 p_1^\nu p_2^\mu + f_4 p_2^\mu p_2^\nu \\
& + f_5 \gamma^\nu p_1^\mu + f_6 \gamma^\mu p_1^\nu + f_7 \gamma^\nu p_2^\mu + f_8 \gamma^\mu p_2^\nu + f_9 \gamma^\mu \gamma^\nu + f_{10} \gamma^\nu \gamma^\mu + f_{11} \not{p}_3 p_1^\mu p_1^\nu \\
& + f_{12} \not{p}_3 p_1^\mu p_2^\nu + f_{13} \not{p}_3 p_1^\nu p_2^\mu + f_{14} \not{p}_3 p_2^\mu p_2^\nu + f_{15} \not{p}_3 \gamma^\nu p_1^\mu + f_{16} \not{p}_3 \gamma^\mu p_1^\nu + f_{17} \not{p}_3 \gamma^\nu p_2^\mu \\
& + f_{18} \not{p}_3 \gamma^\mu p_2^\nu + f_{19} \not{p}_3 \gamma^\mu \gamma^\nu + f_{20} \not{p}_3 \gamma^\nu \gamma^\mu + f'_1 \gamma_5 p_1^\mu p_1^\nu + f'_2 \gamma_5 p_1^\mu p_2^\nu + f'_3 \gamma_5 p_1^\nu p_2^\mu \\
& + f'_4 \gamma_5 p_2^\mu p_2^\nu + f'_5 \gamma_5 \gamma^\nu p_1^\mu + f'_6 \gamma_5 \gamma^\mu p_1^\nu + f'_7 \gamma_5 \gamma^\nu p_2^\mu + f'_8 \gamma_5 \gamma^\mu p_2^\nu + f'_9 \gamma_5 \gamma^\mu \gamma^\nu \\
& + f'_{10} \gamma_5 \gamma^\nu \gamma^\mu + f'_{11} \gamma_5 \not{p}_3 p_1^\mu p_1^\nu + f'_{12} \gamma_5 \not{p}_3 p_1^\mu p_2^\nu + f'_{13} \gamma_5 \not{p}_3 p_1^\nu p_2^\mu + f'_{14} \gamma_5 \not{p}_3 p_2^\mu p_2^\nu \\
& + f'_{15} \gamma_5 \not{p}_3 \gamma^\nu p_1^\mu + f'_{16} \gamma_5 \not{p}_3 \gamma^\mu p_1^\nu + f'_{17} \gamma_5 \not{p}_3 \gamma^\nu p_2^\mu \\
& + f'_{18} \gamma_5 \not{p}_3 \gamma^\mu p_2^\nu + f'_{19} \gamma_5 \not{p}_3 \gamma^\mu \gamma^\nu + f'_{20} \gamma_5 \not{p}_3 \gamma^\nu \gamma^\mu) v(p_2),
\end{aligned} \tag{A.2}$$

where the f_i s and f'_i s are expressed explicitly as,

$$\begin{aligned}
f'_1 = & -36(m_b^2 D_{13} + m_t^2 (D_{26} + D_{38})) \\
& -m_t m_c (D_{25} + D_{310}) [p_2, -p_4, -p_3, m_b, M_s, M_s, M_s] \\
& + 12(m_b^2 (D_{11} - D_{12}) + m_t m_c (D_{25} - D_{26} - D_{310} + D_{35})) \\
& + m_t^2 (D_{21} - D_{24} + D_{31} - D_{34}) [-p_1, p_3, -p_2, m_b, M_s, M_s, m_b] \\
& - 4(m_b^2 (D_{22} - D_{24}) - m_t m_c (D_{310} - D_{38})) \\
& + m_t^2 (D_{32} - D_{36}) [p_3, -p_1, -p_2, m_b, m_b, M_s, m_b],
\end{aligned} \tag{A.3}$$

$$\begin{aligned}
f_1 = & f'_1(m_i^2 \rightarrow -m_i^2, i = b, t) + 32m_t^2 (D_{11} - D_{12} + 2D_{21} - 2D_{24} \\
& - 2D_{25} + 2D_{26} + D_{31} + 2D_{310} - D_{34} - 2D_{35} \\
& + D_{37} - D_{39}) [p_1, -p_3, -p_4, M_s, m_t, m_t, m_t],
\end{aligned} \tag{A.4}$$

$$\begin{aligned}
f'_2 = & 24a_1 (m_b^2 C_0 - m_t m_c (C_{11} + C_{21}) + m_t^2 (C_{12} + C_{23})) [p_2, -p_4, m_b, M_s, M_s] \\
& - 24a_1 (m_b^2 C_0 - m_t m_c C_{22} + m_t^2 (C_{12} + C_{23})) [-p_4, p_2, m_b, m_b, M_s] \\
& - 36(m_b^2 (D_0 - D_{13}) + m_t m_c (D_{11} + D_{21} - D_{25} - D_{310} + D_{34})) \\
& + m_t^2 (D_{12} + D_{22} + D_{24} - D_{26} + D_{36} - D_{38}) [p_2, -p_4, -p_3, m_b, M_s, M_s, M_s] \\
& - 12(m_b^2 (D_0 + D_{12}) - m_t m_c (D_{23} - D_{26} - D_{310} + D_{37}) + m_t^2 (D_{11} - D_{13} + D_{21} \\
& + D_{24} - 2D_{25} + D_{34} + D_{35})) [-p_1, p_3, -p_2, m_b, M_s, M_s, m_b] \\
& + 4(m_b^2 (D_{12} + D_{24}) + m_t m_c (D_{310} - D_{39})) \\
& + m_t^2 (D_{22} - D_{26} + D_{36} - D_{38}) [p_3, -p_1, -p_2, m_b, m_b, M_s, m_b],
\end{aligned} \tag{A.5}$$

$$\begin{aligned}
f_2 = & f'_2(m_i^2 \rightarrow -m_i^2, i = b, t) + 32a_1 m_t (m_c (C_{11} + C_{21}) \\
& + m_t (C_{12} + C_{23})) [-p_2, p_4, M_s, m_t, m_t] - 32m_t^2 (D_{12} - D_{13} + D_{23} + 2D_{24} \\
& - D_{25} - 2D_{26} - 2D_{310} + D_{34} + D_{39}) [p_1, -p_3, -p_4, M_s, m_t, m_t, m_t],
\end{aligned} \tag{A.6}$$

$$\begin{aligned}
f'_3 = & 36(m_b^2(D_{25} - D_{26}) + m_t m_c D_{35} \\
& - m_t^2(D_{310} - D_{38})) [p_2, -p_4, -p_3, m_b, M_s, M_s, M_s] + 12(m_b^2(D_{25} - D_{26}) \\
& + m_t m_c(D_{37} - D_{39}) - m_t^2(D_{310} - D_{35})) [-p_1, p_3, -p_2, m_b, M_s, M_s, m_b] \\
& + 4(m_b^2(D_{25} - D_{26}) + m_t m_c(D_{37} - D_{39}) \\
& + m_t^2(D_{310} - D_{38})) [p_3, -p_1, -p_2, m_b, m_b, M_s, m_b],
\end{aligned} \tag{A.7}$$

$$\begin{aligned}
f_3 = & f'_3(m_i^2 \rightarrow -m_i^2, i = b, t) \\
& + 32m_t^2(D_{37} - D_{39} - D_{25} + D_{26} + D_{310} - D_{35}) [p_1, -p_3, -p_4, M_s, m_t, m_t, m_t],
\end{aligned} \tag{A.8}$$

$$\begin{aligned}
f'_4 = & -36(m_b^2(D_{11} - D_{12} + D_{26}) - m_t m_c(D_{21} + D_{31} - D_{35}) - m_t^2(D_{22} - D_{24} \\
& + D_{310} - D_{34} + D_{36} - D_{38})) [p_2, -p_4, -p_3, m_b, M_s, M_s, M_s] \\
& - 12(m_b^2(D_{13} + D_{26}) - m_t m_c(D_{33} - D_{39}) - m_t^2(D_{23} - D_{25} \\
& - D_{310} + D_{37})) [-p_1, p_3, -p_2, m_b, M_s, M_s, m_b] \\
& + 4(m_b^2(D_{13} + D_{25}) - m_t m_c(D_{33} - D_{37}) \\
& - m_t^2(D_{23} - D_{26} - D_{310} + D_{39})) [p_3, -p_1, -p_2, m_b, m_b, M_s, m_b],
\end{aligned} \tag{A.9}$$

$$\begin{aligned}
f_4 = & f'_4(m_i^2 \rightarrow -m_i^2, i = b, t) + 32m_t^2(D_{26} + D_{310} - D_{23} - D_{39}) [p_1, -p_3, -p_4, M_s, m_t, m_t, m_t],
\end{aligned} \tag{A.10}$$

$$\begin{aligned}
f'_5 = & 8a_2a_3m_t(m_b^2B_0 + m_t^2B_1)[-p_1, m_b, M_s] \\
& + 8a_1a_3m_t(m_b^2B_0 - m_tm_cB_1)[p_2, m_b, M_s] \\
& - 4a_1a_2(m_t(m_b^2B_0 + m_t^2B_1) + 2m_t(p_1 \cdot p_3)B_1)[-p_1 + p_3, m_t, M_s] \\
& + 12a_2m_t((m_b^2C_0 + m_t^2(C_{11} + C_{21}))) \\
& + 2(C_{24} + (p_1 \cdot p_3)(C_{12} + C_{23}))[-p_1, p_3, m_b, M_s, M_s] \\
& - 24a_1m_tC_{24}[p_2, -p_4, m_b, M_s, M_s] - 12a_2m_t(2C_{24} + m_b^2(C_0 + C_{12})) \\
& - m_tm_cC_{22}[p_3, -p_1, m_b, m_b, M_s] + 12a_1m_t(2m_b^2C_0 - 2C_{24} \\
& + m_c^2(C_{22} - C_{23}) - m_tm_cC_{12} + m_t^2(C_{11} + C_{21})) \\
& + 2(p_1 \cdot p_2 - p_2 \cdot p_3)(C_{11} - C_{12} + C_{21} - C_{23}) \\
& - 2p_1 \cdot p_3(C_{11} + C_{21}))[-p_4, p_2, m_b, m_b, M_s] \\
& - 36m_t(D_{27} + D_{312})[p_2, -p_4, -p_3, m_b, M_s, M_s, M_s] + 6(m_t(4D_{27} + 4D_{311} \\
& + m_c^2(D_{23} + D_{37}) + m_tm_c(D_{13} + D_{25}) + m_t^2(D_{11} - D_{21} \\
& - D_{31})) - 2m_t((p_1 \cdot p_2)(D_{13} + 2D_{25} + D_{35}) + (p_1 \cdot p_3)(D_{12} + D_{24} + D_{34}) \\
& + (p_2 \cdot p_3)(D_{13} + D_{25} + D_{26} + D_{310})))[-p_1, p_3, -p_2, m_b, M_s, M_s, m_b] \\
& - 2(m_t(2D_{27} + 2D_{312} + m_b^2D_0 - m_c^2D_{23} - m_tm_c(D_{22} - D_{26})) \\
& + m_b^2m_tD_{12} + 2m_t(p_2 \cdot p_3)(D_{25} - D_{26}))[p_3, -p_1, -p_2, m_b, m_b, M_s, m_b],
\end{aligned} \tag{A.11}$$

$$\begin{aligned}
f_5 = & f'_5(m_tm_c \rightarrow -m_tm_c) - 16a_2a_3m_t^3B_1[-p_1, m_t, M_s] + 16a_1a_2m_t(2p_1 \cdot p_3 \\
& - m_t^2)B_1[-p_1 + p_3, m_t, M_s] + 16a_1a_3m_t^2m_cB_1[p_2, m_t, M_s] \\
& - 16a_2m_t(m_t^2C_0 + m_tm_c(2C_{11} + C_{21})) \\
& + 2C_{24}[p_1, -p_3, M_s, m_t, m_t] - 16a_1m_t(2C_{24} - m_c^2(C_{12} + C_{22} - C_0) - 2(p_1 \cdot p_2 \\
& - p_2 \cdot p_3)(C_{22} - C_{23}) - 2p_1 \cdot p_3(C_{12} + C_{22})))[-p_2, p_4, M_s, m_t, m_t] \\
& - 16m_t(2D_{311} - 2D_{313} - m_tm_c(D_{21} - D_{25}) - m_t^2(D_0 + 2D_{11} - D_{13}) \\
& - 2(p_2 \cdot p_3)(D_{25} - D_{26}))[p_1, -p_3, -p_4, M_s, m_t, m_t],
\end{aligned} \tag{A.12}$$

$$\begin{aligned}
f'_6 = & -36m_tD_{313}[p_2, -p_4, -p_3, m_b, M_s, M_s, M_s] + 12m_t(D_{311} \\
& - D_{312})[-p_1, p_3, -p_2, m_b, M_s, M_s, m_b] - 2(m_t(4D_{311} - 4D_{312} + m_b^2(D_{11} - D_{12})) \\
& - m_c^2(D_{37} - D_{39}) + m_t^2(D_{32} - D_{36})) - 2m_t(p_1 \cdot p_2(D_{310} - D_{38}) + p_1 \cdot p_3(D_{22} - D_{24} \\
& - D_{34} + D_{36}) + p_2 \cdot p_3(D_{310} - D_{35}))[p_3, -p_1, -p_2, m_b, m_b, M_s, m_b],
\end{aligned} \tag{A.13}$$

$$\begin{aligned}
f_6 = & f'_6 + 16m_t(4D_{311} - 4D_{312} - m_t^2(2D_{21} - 2D_{24} - 2D_{25} + 2D_{26} + D_{31} + 2D_{310} \\
& - D_{34} - 2D_{35} + D_{37} - D_{39}) + 2(p_1 \cdot p_2)(D_{25} - D_{26} - D_{310} + D_{35} - D_{37} + D_{39}) \\
& - 2(p_1 \cdot p_3)(D_{22} - D_{24} + D_{25} - D_{26} - D_{34} + D_{35} + D_{36} - D_{37} - D_{38} + D_{39}) \\
& - 2(p_2 \cdot p_3)(D_{25} - D_{26} + D_{310} - D_{37} - D_{38} + D_{39))[p_1, -p_3, -p_4, M_s, m_t, m_t, m_t],
\end{aligned} \tag{A.14}$$

$$\begin{aligned}
f'_7 = & -36m_t(D_{312} - D_{311})[p_2, -p_4, -p_3, m_b, M_s, M_s, M_s] - 6(m_t(4D_{313} \\
& - m_c^2 D_{33} - m_t m_c D_{23} - m_t^2(D_{25} + D_{35})) - m_b^2 m_c D_{13} \\
& - 2m_t(p_1 \cdot p_2(D_{23} + D_{37}) - p_1 \cdot p_3(D_{26} + D_{310}) \\
& - p_2 \cdot p_3(D_{23} + D_{39})))[-p_1, p_3, -p_2, m_b, M_s, M_s, m_b] \\
& + 2(m_t(4D_{313} - m_c^2 D_{33} - m_t m_c D_{23} - m_t^2(D_{26} + D_{38})) - m_b^2 m_c D_{13} \\
& + 2m_t(p_1 \cdot p_2(D_{23} + D_{39}) + p_1 \cdot p_3(D_{25} + D_{310}) \\
& + p_2 \cdot p_3(D_{23} + D_{37}))) [p_3, -p_1, -p_2, m_b, m_b, M_s, m_b],
\end{aligned} \tag{A.15}$$

$$\begin{aligned}
f_7 = & f'_7(m_t m_c \rightarrow -m_t m_c) + 16m_t(m_t^2(-D_{13} - D_{23} + D_{25} + D_{33} + D_{35} - 2D_{37}) \\
& - 4D_{313} + 2(p_1 \cdot p_2)(D_{33} - D_{37}) + 2(p_1 \cdot p_3)(D_{23} - D_{25} - D_{310} - D_{33} \\
& + D_{37} + D_{39}) - 2(p_2 \cdot p_3)(D_{33} - D_{39})) [p_1, -p_3, -p_4, M_s, m_t, m_t, m_t],
\end{aligned} \tag{A.16}$$

$$\begin{aligned}
f'_8 = & 24a_1 m_t(p_1 \cdot p_3)(C_{12} + C_{23})[p_2, -p_4, m_b, M_s, M_s] \\
& - 24a_1 m_t(p_1 \cdot p_3)(C_{12} + C_{23})[-p_4, p_2, m_b, m_b, M_s] \\
& - 36m_t(D_{313} - D_{27} - D_{311})[p_2, -p_4, -p_3, m_b, M_s, M_s, M_s] \\
& - 12m_t(D_{27} + D_{312} - D_{313})[-p_1, p_3, -p_2, m_b, M_s, M_s, m_b] \\
& - 2(m_t(2D_{27} + 4D_{311} + 2D_{313} + m_b^2(D_0 + D_{11}) - m_c^2(D_{23} + D_{37}) - m_t^2(D_{22} + D_{36}) \\
& - 2m_t(p_1 \cdot p_2(D_{26} + D_{310}) - p_1 \cdot p_3(D_{12} - D_{13} + 2D_{24} - D_{26} + D_{34}) \\
& - p_2 \cdot p_3(D_{25} + D_{35}))) [p_3, -p_1, -p_2, m_b, m_b, M_s, m_b],
\end{aligned} \tag{A.17}$$

$$\begin{aligned}
f_8 = & f'_8 - 32a_1 m_t(p_1 \cdot p_3)C_{12}[-p_2, p_4, M_s, m_t, m_t] + 16m_t(6D_{313} - 2D_{27} \\
& - 4D_{312} + m_t^2(2D_{23} + 2D_{24} - 2D_{25} - 2D_{26} - 2D_{310} \\
& - D_{33} + D_{34} - D_{35} + 2D_{37} + D_{39}) + 2(p_1 \cdot p_2)(D_{23} - D_{26} - D_{310} - D_{33} + D_{37} + D_{39}) \\
& + 2(p_1 \cdot p_3)(D_{25} - D_{22} - 2D_{23} + 2D_{26} + 2D_{310} + D_{33} - D_{36} - D_{37} + D_{38} - 2D_{39}) \\
& + 2(p_2 \cdot p_3)(D_{26} - D_{23} + D_{33} + D_{38} - 2D_{39}) [p_1, -p_3, -p_4, M_s, m_t, m_t, m_t],
\end{aligned} \tag{A.18}$$

$$\begin{aligned}
f'_9 = & 4a_2a_3m_t^2(m_b^2B_0 - m_t^2B_1)[-p_1, m_b, M_s] \\
& +4a_1a_2(p_1 \cdot p_3)(m_tm_cB_1 - m_b^2B_0)[-p_1 + p_3, m_b, M_s] \\
& -12a_2m_t^2C_{24}[-p_1, p_3, m_b, M_s, M_s] - 6a_2m_t^2(2C_{24} + m_b^2C_0 - m_t^2C_{22}) \\
& -2(p_1 \cdot p_3)(m_b^2C_0 - m_c^2C_{12} - m_t^2C_{23})[p_3, -p_1, m_b, m_b, M_s] \\
& -12a_1m_tm_c(p_1 \cdot p_3)C_0[-p_4, p_2, m_b, m_b, M_s] \\
& +18(m_b^2D_{27} - m_tm_cD_{311} + m_t^2D_{312})[p_2, -p_4, -p_3, m_b, M_s, M_s, M_s] \\
& -6(m_tm_cD_{313} + m_t^2(D_{27} + D_{311}))[-p_1, p_3, -p_2, m_b, M_s, M_s, m_b] \\
& -(2m_b^2D_{27} + m_b^4D_0 - m_b^2m_c^2D_{23} - m_b^2m_t^2D_{22} + m_tm_c(2D_{27} + 4D_{313} + m_b^2(D_0 + D_{13})) \\
& -m_c^2(D_{23} + D_{33}) - m_t^2(D_{22} + D_{38})) + m_t^2(2D_{27} + 4D_{312} + m_b^2(D_0 + D_{12})) \\
& -m_c^2(D_{23} + D_{39}) - m_t^2(D_{22} + D_{32})) + 2m_b^2(p_1 \cdot p_2D_{26} - p_1 \cdot p_3(D_0 - D_{24}) + p_2 \cdot p_3D_{25}) \\
& -2(p_1 \cdot p_2(m_tm_cD_{39} + m_t^2(D_{26} + D_{38})) - p_1 \cdot p_3(m_tm_c(D_{12} - D_{13} + D_{310}) \\
& + m_t^2(D_{24} + D_{36})) - p_2 \cdot p_3(m_tm_cD_{37} + m_t^2(D_{25} + D_{310}))) [p_3, -p_1, -p_2, m_b, m_b, M_s, m_b], \tag{A.19}
\end{aligned}$$

$$\begin{aligned}
f_9 = & -f'_9(m_tm_c \rightarrow -m_tm_c) \\
& +8a_2a_3m_t^4B_1[-p_1, m_t, M_s] + 16a_1a_2m_tm_c(p_1 \cdot p_3)B_1[-p_1 + p_3, m_t, M_s] \\
& +8a_2m_t^2(2C_{24} + m_t^2(2C_{11} + C_{21}) + 2(p_1 \cdot p_3)(C_0 + C_{11} \\
& + C_{12} + C_{23}))[p_1, -p_3, M_s, m_t, m_t] + 16a_1(p_1 \cdot p_3)m_tm_c(C_0 \\
& + C_{11})[-p_2, p_4, M_s, m_t, m_t] + 4m_t(4m_t(D_{27} + 2D_{311} - 2D_{313}) \\
& - 4m_cm_t^2(D_{11} - D_{13}) - m_t^3(4D_{21} + 4D_{23} - 8D_{25} + 2D_{31} - 2D_{33} \\
& - 6D_{35} + 6D_{37}) + 4(p_1 \cdot p_2)(m_cD_{13} - m_t(D_{23} - D_{25} - D_{33} \\
& - D_{35} + 2D_{37})) + 4(p_1 \cdot p_3)(m_cD_{12} + m_t(D_{11} - D_{13} \\
& + D_{21} + 2D_{23} + D_{24} - 3D_{25} - D_{26} - 2D_{310} - D_{33} + D_{34} - D_{35} \\
& + 2D_{37} + D_{39})) - 4(p_2 \cdot p_3)(m_cD_{13} - m_t(D_{23} - D_{25} \\
& - D_{26} - D_{310} - D_{33} + D_{37} + D_{39}))) [p_1, -p_3, -p_4, M_s, m_t, m_t, m_t], \tag{A.20}
\end{aligned}$$

$$\begin{aligned}
f'_{10} = & 18(m_b^2D_{27} - m_tm_cD_{311} + m_t^2D_{312})[p_2, -p_4, -p_3, m_b, M_s, M_s, M_s] \\
& -6(m_b^2D_{27} + m_tm_cD_{313} + m_t^2D_{311})[-p_1, p_3, -p_2, m_b, M_s, M_s, m_b] \\
& +2(m_b^2D_{27} + m_tm_cD_{313} + m_t^2D_{312})[p_3, -p_1, -p_2, m_b, m_b, M_s, m_b], \tag{A.21}
\end{aligned}$$

$$\begin{aligned}
f_{10} = & f'_{10}(m_i^2 \rightarrow -m_i^2, i = b, t) \\
& -16m_t^2(D_{27} + D_{311} - D_{313})[p_1, -p_3, -p_4, M_s, m_t, m_t, m_t], \tag{A.22}
\end{aligned}$$

$$\begin{aligned}
f'_{11} = & 36m_t(D_{23} - D_{26} - D_{38} + D_{39})[p_2, -p_4, -p_3, m_b, M_s, M_s, M_s] \\
& -12m_t(D_{22} - D_{24} - D_{34} + D_{36})[-p_1, p_3, -p_2, m_b, M_s, M_s, m_b] \\
& -4m_t(D_{22} - D_{24} - D_{34} + D_{36})[p_3, -p_1, -p_2, m_b, m_b, M_s, m_b], \tag{A.23}
\end{aligned}$$

$$f_{11} = f'_{11} + 32m_t(D_{22} - D_{24} + D_{25} - D_{26} - D_{34} + D_{35} + D_{36} - D_{37} - D_{38} + D_{39})[p_1, -p_3, -p_4, M_s, m_t, m_t, m_t], \quad (\text{A.24})$$

$$\begin{aligned} f'_{12} = & 36m_t(D_{12} - D_{13} + D_{22} + D_{23} + D_{24} - D_{25} - 2D_{26} - D_{310} + D_{36} \\ & - D_{38} + D_{39})[p_2, -p_4, -p_3, m_b, M_s, M_s, M_s] - 12m_t(D_{12} - D_{13} + D_{22} \\ & + D_{24} - D_{25} - D_{26} - D_{310} + D_{36})[-p_1, p_3, -p_2, m_b, M_s, M_s, m_b] \\ & + 4m_t(D_{12} - D_{13} + 2D_{24} - 2D_{26} - D_{310} + D_{34})[p_3, -p_1, -p_2, m_b, m_b, M_s, m_b], \end{aligned} \quad (\text{A.25})$$

$$f_{12} = f'_{12} + 32m_t(D_{22} + D_{23} - D_{25} - D_{26} - D_{310} + D_{36} - D_{38} + D_{39})[p_1, -p_3, -p_4, M_s, m_t, m_t, m_t], \quad (\text{A.26})$$

$$\begin{aligned} f'_{13} = & 36m_t(D_{310} - D_{37} - D_{38} + D_{39})[p_2, -p_4, -p_3, m_b, M_s, M_s, M_s] \\ & + 12m_t(D_{310} - D_{38})[-p_1, p_3, -p_2, m_b, M_s, M_s, m_b] \\ & - 4m_t(D_{310} - D_{35})[p_3, -p_1, -p_2, m_b, m_b, M_s, m_b], \end{aligned} \quad (\text{A.27})$$

$$f_{13} = f'_{13} + 32m_t(D_{25} - D_{26} + D_{310} - D_{37} - D_{38} + D_{39})[p_1, -p_3, -p_4, M_s, m_t, m_t, m_t], \quad (\text{A.28})$$

$$\begin{aligned} f'_{14} = & 36m_t(D_{22} - D_{24} + D_{25} - D_{26} - D_{34} \\ & + D_{35} + D_{36} - D_{37} - D_{38} + D_{39})[p_2, -p_4, -p_3, m_b, M_s, M_s, M_s] \\ & + 12m_t(D_{23} - D_{26} - D_{38} + D_{39})[-p_1, p_3, -p_2, m_b, M_s, M_s, m_b] \\ & - 4m_t(D_{23} - D_{25} - D_{35} + D_{37})[p_3, -p_1, -p_2, m_b, m_b, M_s, m_b], \end{aligned} \quad (\text{A.29})$$

$$f_{14} = f'_{14} + 32m_t(D_{23} - D_{26} - D_{38} + D_{39})[p_1, -p_3, -p_4, M_s, m_t, m_t, m_t], \quad (\text{A.30})$$

$$\begin{aligned} f'_{15} = & 12a_2(m_b^2 C_0 + m_t^2(C_{11} + C_{21} - C_{12} - C_{23}))[-p_1, p_3, m_b, M_s, M_s] \\ & - 12a_2(m_b^2 C_0 - m_t m_c C_{12} - m_t^2(C_{23} - C_{22})) [p_3, -p_1, m_b, m_b, M_s] \\ & + 6(m_b^2 D_0 + m_t m_c(D_{13} + D_{25})) \\ & + m_t^2(D_{11} - D_{12} + D_{21} - D_{24})[-p_1, p_3, -p_2, m_b, M_s, M_s, m_b] \\ & - 2(m_b^2 D_0 - m_t m_c(D_{12} - D_{13} - D_{26})) \\ & + m_t^2(D_{22} + D_{24})[p_3, -p_1, -p_2, m_b, m_b, M_s, m_b], \end{aligned} \quad (\text{A.31})$$

$$\begin{aligned}
f_{15} = & f'_{15}(m_i^2 \rightarrow -m_i^2, i = b, t) \\
& + 16a_2 m_t^2 (C_{11} + C_{21} - C_{12} - C_{23}) [p_1, -p_3, M_s, m_t, m_t] + 16m_t (m_c D_{13} \\
& - m_t (D_{11} - D_{12} + D_{21} - D_{24} - D_{25} + D_{26})) [p_1, -p_3, -p_4, M_s, m_t, m_t, m_t],
\end{aligned} \tag{A.32}$$

$$\begin{aligned}
f'_{16} = & -2(m_b^2 (D_{11} - D_{12}) + m_t m_c (D_{25} - D_{26}) \\
& - m_t^2 (D_{22} - D_{24})) [p_3, -p_1, -p_2, m_b, m_b, M_s, m_b],
\end{aligned} \tag{A.33}$$

$$\begin{aligned}
f_{16} = & f'_{16}(m_i^2 \rightarrow -m_i^2, i = b, t) \\
& + 16m_t^2 (D_{11} - D_{12} + D_{21} - D_{24} - D_{25} + D_{26}) [p_1, -p_3, -p_4, M_s, m_t, m_t, m_t],
\end{aligned} \tag{A.34}$$

$$\begin{aligned}
f'_{17} = & 6(m_b^2 D_{13} + m_t m_c D_{23} + m_t^2 (D_{25} - D_{26})) [-p_1, p_3, -p_2, m_b, M_s, M_s, m_b] \\
& - 2(m_b^2 D_{13} + m_t m_c D_{23} - m_t^2 (D_{25} - D_{26})) [p_3, -p_1, -p_2, m_b, m_b, M_s, m_b],
\end{aligned} \tag{A.35}$$

$$\begin{aligned}
f_{17} = & f'_{17}(m_i^2 \rightarrow -m_i^2, i = b, t) \\
& + 16m_t (m_c D_{13} + m_t (D_{25} - D_{26})) [p_1, -p_3, -p_4, M_s, m_t, m_t, m_t],
\end{aligned} \tag{A.36}$$

$$\begin{aligned}
f'_{18} = & 12a_1 (m_b^2 C_0 - m_t m_c (C_{11} + C_{21}) + m_t^2 (C_{12} + C_{23})) [p_2, -p_4, m_b, M_s, M_s] \\
& - 12a_1 (m_b^2 C_0 - m_t m_c C_{22} + m_t^2 (C_{12} + C_{23})) [-p_4, p_2, m_b, m_b, M_s] \\
& - 2(m_b^2 (D_0 + D_{11}) - m_t m_c (D_{23} - D_{25}) \\
& + m_t^2 (D_{12} - D_{13} + D_{24} - D_{26})) [p_3, -p_1, -p_2, m_b, m_b, M_s, m_b],
\end{aligned} \tag{A.37}$$

$$\begin{aligned}
f_{18} = & f'_{18}(m_i^2 \rightarrow -m_i^2, i = b, t) \\
& - 16a_1 m_t (m_c (C_{12} - C_{21} + C_{23}) - m_t C_{11}) [-p_2, p_4, M_s, m_t, m_t] \\
& - 16m_t^2 (D_{12} + D_{24} - D_{13} - D_{26}) [p_1, -p_3, -p_4, M_s, m_t, m_t, m_t],
\end{aligned} \tag{A.38}$$

$$\begin{aligned}
f'_{19} = & 4a_2a_3m_t(m_b^2B_0 + m_t^2B_1)[-p_1, m_b, M_s] + 4a_1a_3m_t(m_b^2B_0 - m_tm_cB_1)[p_2, m_b, M_s] \\
& - 2a_1a_2m_t(m_b^2B_0 + m_t^2B_1 - 2(p_1 \cdot p_3)B_1)[-p_1 + p_3, m_b, M_s] \\
& - 12a_2m_tC_{24}[-p_1, p_3, m_b, M_s, M_s] - 12a_1m_tC_{24}[p_2, -p_4, m_b, M_s, M_s] \\
& - 6a_2m_t(2C_{24} + m_t^2(C_{12} - C_{22}) + 2(p_1 \cdot p_3)(C_{12} + C_{23}))[p_3, -p_1, m_b, m_b, M_s] \\
& + 6a_1(2m_b^2m_tC_0 - m_t(2C_{24} - m_c^2(C_{22} - C_{23}) + m_tm_cC_{12} - m_t^2(C_{11} + C_{21})) \\
& + 2m_t(p_1 \cdot p_2 - p_2 \cdot p_3)(C_{11} - C_{12} + C_{21} - C_{23}) \\
& - 2m_t(p_1 \cdot p_3)(C_{11} + C_{21}))[-p_4, p_2, m_b, m_b, M_s] \\
& - 18m_t(D_{313} - D_{312})D_0[p_2, -p_4, -p_3, m_b, M_s, M_s, M_s] - (m_t(4D_{27} + 4D_{311} \\
& + m_b^2(D_0 + D_{11}) - m_c^2(2D_{23} + d37) - m_tm_cD_{13} - m_t^2(D_{12} + 2D_{22} + d36)) \\
& + m_b^2m_tD_0 - 2m_t(p_1 \cdot p_2(D_{13} + 2D_{26} + D_{310}) - p_1 \cdot p_3(D_{12} + 2D_{24} + D_{34}) \\
& - p_2 \cdot p_3(D_{13} + 2D_{25} + D_{35}))) [p_3, -p_1, -p_2, m_b, m_b, M_s, m_b] \\
& - 6m_t(D_{27} - D_{312})[-p_1, p_3, -p_2, m_b, M_s, M_s, m_b]
\end{aligned} \tag{A.39}$$

$$\begin{aligned}
f_{19} = & f'_{19}(m_tm_c \rightarrow -m_tm_c) - 8a_2a_3m_t^3B_1[-p_1, m_t, M_s] + 8a_1a_2m_t(2p_1 \cdot p_3 \\
& - m_t^2)B_1[-p_1 + p_3, m_t, M_s] + 8a_1a_3m_t^2m_cB_1[p_2, m_t, M_s] \\
& - 8a_2m_t(2C_{24} + m_t^2(C_0 - C_{11} - C_{21}) \\
& + 2(p_1 \cdot p_3)(C_{12} + C_{23}))[p_1, -p_3, M_s, m_t, m_t] - 8a_1m_t(2C_{24} - m_c^2(C_{21} - 2C_{23}) \\
& + m_tm_cC_{11} - m_t^2(C_{12} + C_{22} - C_0) - 2(p_1 \cdot p_2 - p_2 \cdot p_3)(C_{22} - C_{23}) \\
& + 2(p_1 \cdot p_3)(C_{12} + C_{22}))[-p_2, p_4, M_s, m_t, m_t] - 8m_t(4D_{312} - 4D_{313} \\
& + m_c^2D_{33} - m_t^2(D_0 - D_{11} + D_{13} - D_{21} + D_{23} + 2D_{24} - 2D_{26} - 2D_{310} \\
& - D_{33} + D_{34} - D_{35} + 2D_{37} + D_{39}) - 2(p_1 \cdot p_2)(D_{25} - D_{26} - D_{310} - D_{33} + D_{37} + D_{39}) \\
& + 2(p_1 \cdot p_3)(D_{22} + D_{23} - 2D_{26} - 2D_{310} - D_{33} + D_{36} + D_{37} - D_{38} + 2D_{39}) \\
& - 2(p_2 \cdot p_3)(D_{33} + D_{38} - 2D_{39}))[p_1, -p_3, -p_4, M_s, m_t, m_t, m_t],
\end{aligned} \tag{A.40}$$

$$\begin{aligned}
f'_{20} = & -18m_t(D_{313} - D_{312})[p_2, -p_4, -p_3, m_b, M_s, M_s, M_s] \\
& - 6m_tD_{312}[-p_1, p_3, -p_2, m_b, M_s, M_s, m_b] + 2m_tD_{311}[p_3, -p_1, -p_2, m_b, m_b, M_s, m_b],
\end{aligned} \tag{A.41}$$

$$f_{20} = f'_{20} + 16m_t(D_{27} + D_{312} - D_{313})[p_1, -p_3, -p_4, M_s, m_t, m_t, m_t], \tag{A.42}$$

where

$$a_1 = \frac{1}{\hat{t} - m_t^2}, \quad a_2 = \frac{1}{\hat{t} - m_c^2} \quad \text{and} \quad a_3 = \frac{1}{m_t^2 - m_c^2}.$$

$$M^{\hat{u}} = M^{\hat{t}} \quad (p_3 \leftrightarrow p_4, \quad \mu \leftrightarrow \nu, \hat{t} \leftrightarrow \hat{u}) \quad (A.43)$$

References

- [1] S. L. Glashow and S. Weinberg, Phys. Rev. **D15**, 1958(1977)
- [2] CDF Collaboration, F. Abe et al., Phys. Rev. Lett. **74**, 2626(1995); D0 Collaboration, S. Abachi et al., *ibid.* **74**,2632(1995); P.C. Bhat, for the D0 collaboration, talk presented at the Wine and Cheese Seminar at Fermilab, February 1997.
- [3] A. Antaramian, L. J. Hall and A. Rasin, Phys. Rev. Lett. **69**, 1871(1992).
- [4] D. Chang, W. S. Hou and W. Y. Keung, CERN preprint CERN-TH. 6795/93(1993).
- [5] T. P. Cheng and M. Sher, Phys. Rev. **D35**, 3484(1987); M. Sher and Y. Yuan, *ibid.* **44**, 1461(1991)
- [6] W. S. Hou, Phys. Lett. **B 296**, 179(1992); D. Chang, W. S. Hou and W. Y. Keung, Phys. Rev. **D48**,217(1993).
- [7] David Atwood et al. Phys. Rev. **D53**, 1199(1996).
- [8] Wei-Shu Hou and Guey-Lin Lin, Phys. Lett. **B379**, 261(1996).
- [9] M. Luke and M. J. Savage, Phys. Lett. **B207**, 387(1993).
- [10] W. S. Hou, Phys. Lett. **B 296**, 179(1992).

- [11] V. Telnov, Nucl. Instrum. Methods **A294**, 72(1990); L. Ginzburg, G. Kotkin and H. Spiesberger, Fortschr. Phys. **34**, 687(1986).
- [12] K. Cheung, Phys. Rev. **D47**, 3750(1993); *ibid.* **50** 1173(1994).
- [13] Particle Data Group, Phys. Rev. **D50**, No. **3**, (1994).
- [14] Kniehl B. A., Phys. Rep. 240(1994)211 and references therein.

Figure Captions

Fig.1 The Feynman diagrams of the subprocess $\gamma\gamma \rightarrow t\bar{c}$.

Fig.2 Total cross sections of the subprocess $\gamma\gamma \rightarrow t\bar{c} + \bar{t}c$ as function of M_s . The solid curve is for $\sqrt{\hat{s}} = 200 GeV$, the dashed curve is for $\sqrt{\hat{s}} = 400 GeV$ and the dotted curve is for $\sqrt{\hat{s}} = 500 GeV$.

Fig.3 Total cross sections of the subprocess $\gamma\gamma \rightarrow t\bar{c} + \bar{t}c$ as function of $\sqrt{\hat{s}}$. The solid curve is for $M_s = 100 GeV$, the dashed curve is for $M_s = 250 GeV$ and the dotted curve is for $M_s = 500 GeV$.

Fig.4 Total cross sections of the process $e^+e^- \rightarrow \gamma\gamma \rightarrow t\bar{c} + \bar{t}c$ as function of \sqrt{s} . The solid curve is for $M_s = 100 GeV$, the dashed curve is for $M_s = 250 GeV$ and the dotted curve is for $M_s = 500 GeV$.

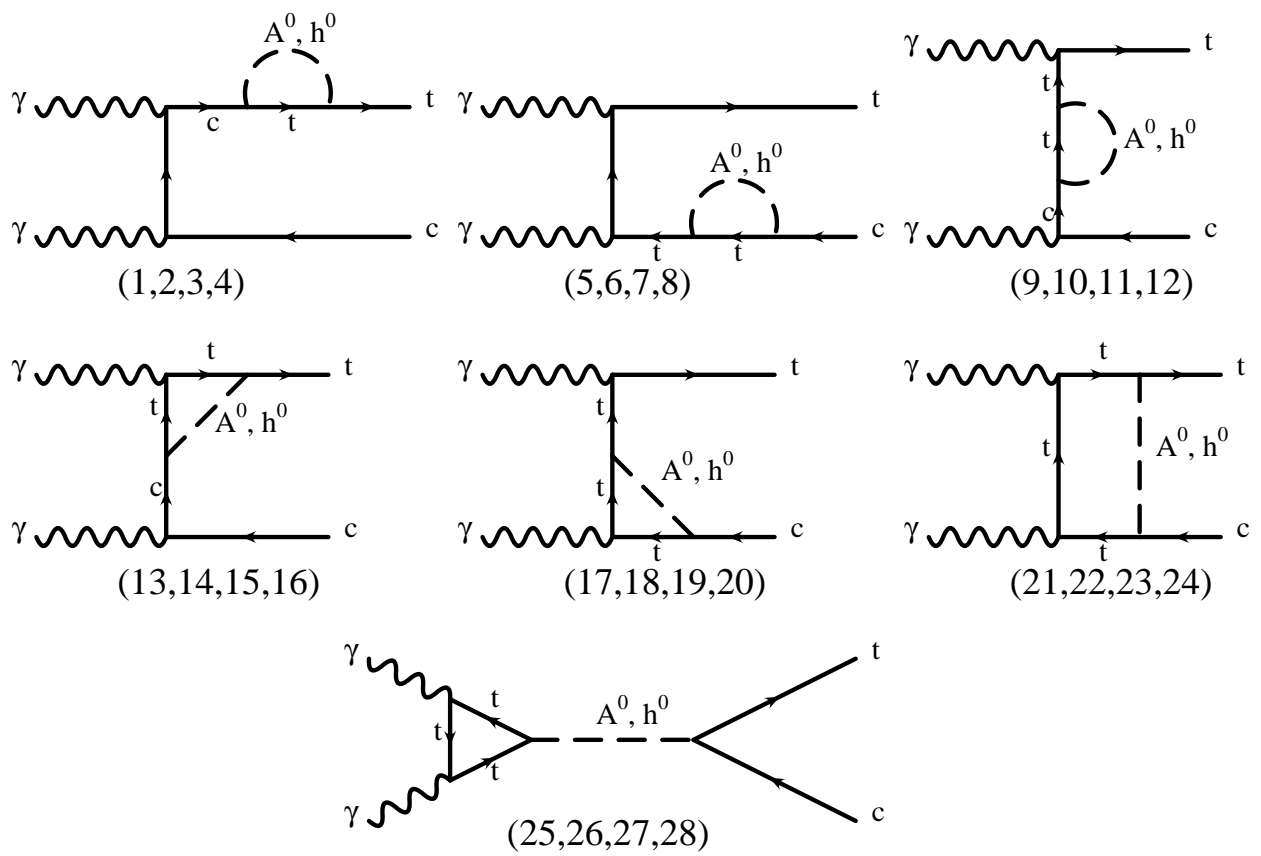


Fig.1 (a)

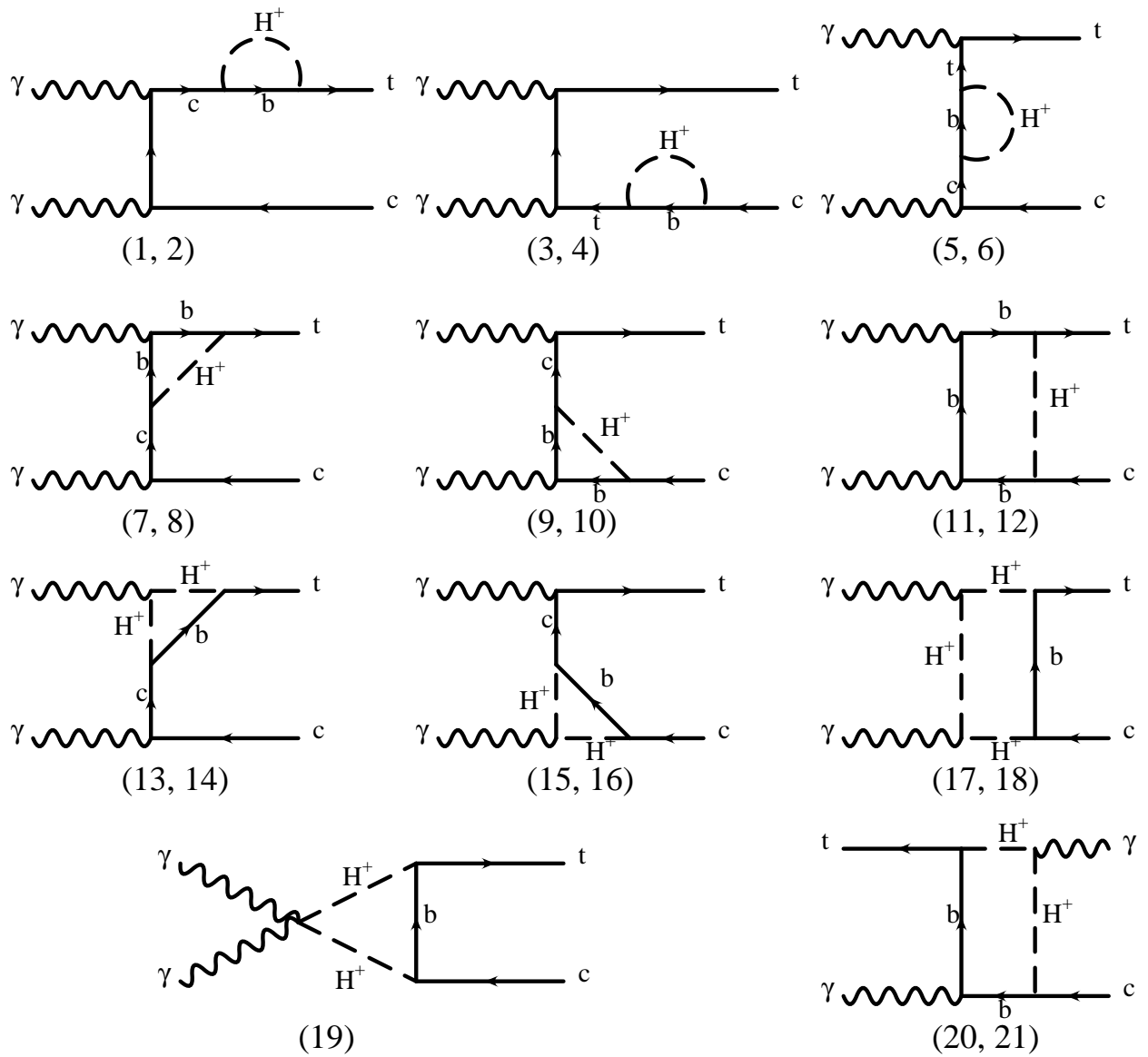


Fig.1 (b)

Fig.2

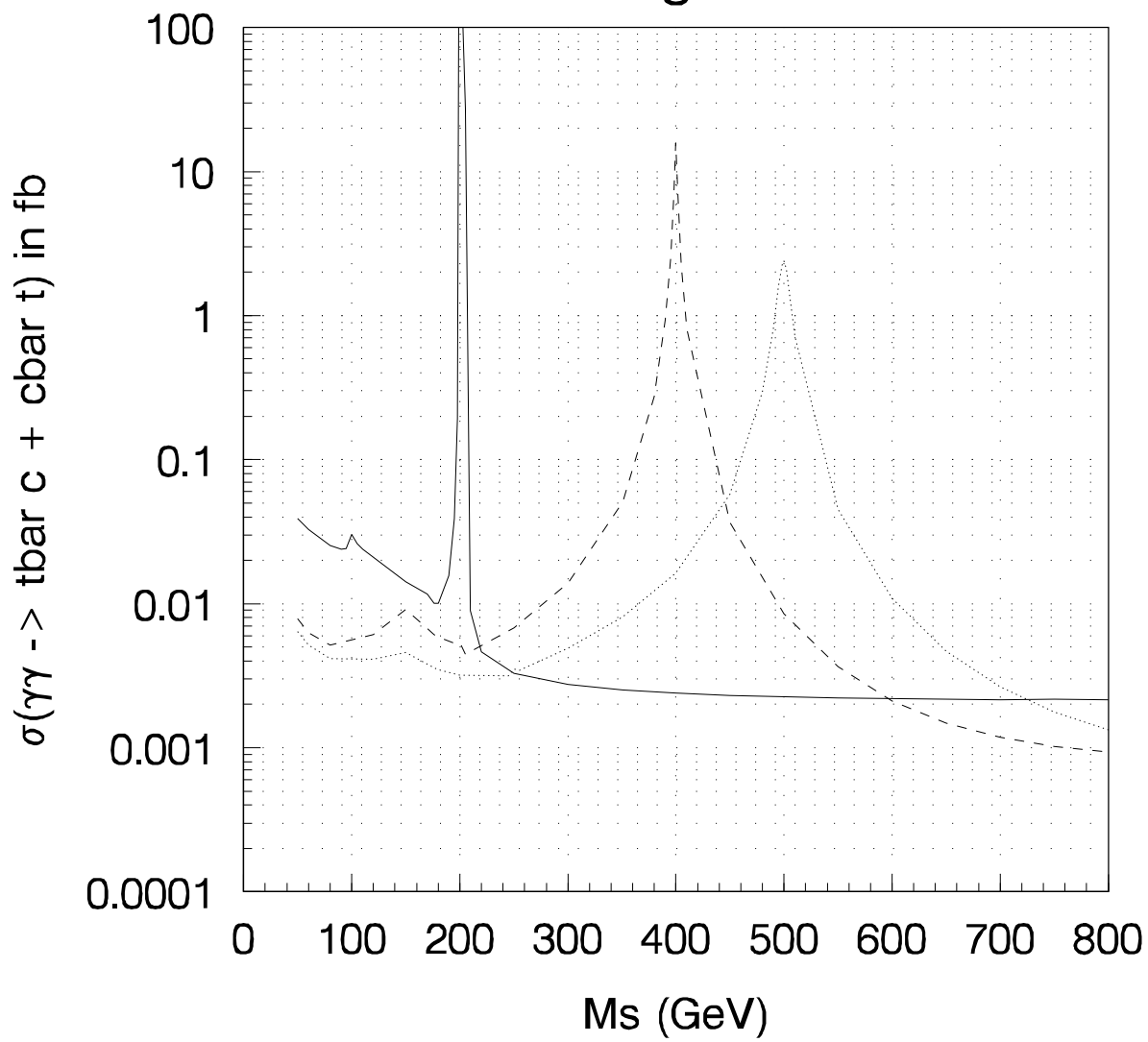


Fig.3

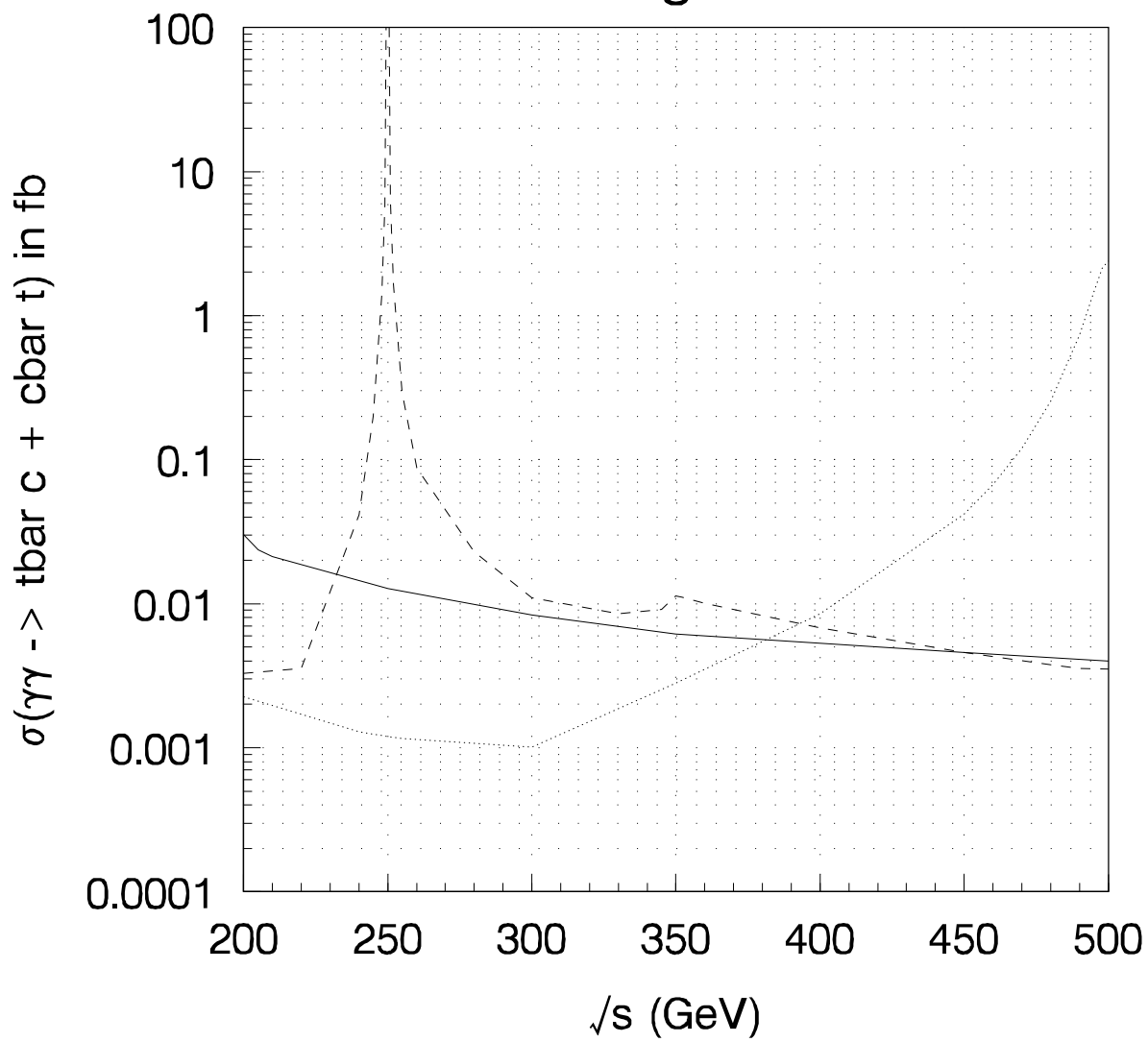


Fig.4

